



High-efficient and Low-cost H₂ Production by Solar-driven Photo-thermo-reforming of Methanol with CuO Catalyst

Donghui Li, Jie Sun,* Rong Ma and Jinjia Wei

Abstract

Solar-driven methanol reforming is recognized as an effective route for hydrogen production considering economic and technological feasibility. However, the currently-available photo-reforming and thermo-reforming suffer from low efficiency and high-cost, respectively. Here, we propose a high-efficient and low-cost reaction system for H₂ production by solar-driven photo-thermo-reforming of methanol to solve this problem with noble-metal-free catalyst of CuO supported on SiO₂ filter. In this system, CuO exhibits excellent hydrogen production performance (100.33 mmol g⁻¹ h⁻¹), and the solar-to-hydrogen efficiency can reach up to 1.85% with 100 mg commercial CuO catalyst. The remarkable performance is attributed to the photo-thermo-catalytic synergism, which is revealed as a self-promoting cycle triggered by in-situ photo reduction of CuO into element Cu and enhanced by the thermally Local Surface Plasmon Resonance (LSPR) effect of element Cu. We hope our work could bring forward to an alternative novel idea for solar-driven H₂ harvesting in the future.

Keywords: Solar energy; Methanol reforming; Hydrogen production; Photo-thermo-synergism.

Received: 14 August 2020; Accepted: 16 September 2020.

Article type: Research article.

1. Introduction

It is extensively believed that hydrogen, as a high energy-density and environmentally-friendly energy carrier, will play an essential role in the future energy world.^[1-3] Since hydrogen is highly light, flammable and metal-embrittling, the currently-available physical-based storage and transportation solutions are generally very energy-consuming and expensive.^[4-6] Therefore, the chemical-based routes are emerging.^[7-9] In recent years, it is generally recognized that methanol is suitable as a promising candidate of high-density, stable and economical hydrogen carrier.^[10,11] With the rising concepts of bio-alcohol^[12] and liquid sunshine,^[13] low-cost and green hydrogen from methanol by solar-driven reforming reaction becomes economically and technologically feasible.^[14] Regrettably, at the moment, it is still a technology far from practical application. One of the main drawbacks concerns the low efficiency reported system.^[15] Thus, it is critical to improve and optimize the solar-driven methanol reforming system in order to forward this technology to be more applicable.^[16] Recently, some noteworthy studies have

been reported that the synergistic effect of photo energy and thermal energy can significantly enhance the performance of light-driven chemical process.^[17-20] Meanwhile, the term “photothermocatalysis” based on the synergistic effect of thermocatalysis and photocatalysis has gradually emerged in researchers’ views.^[21] Although the fundamental mechanism has not yet been fully understood, it has been clearly demonstrated that the performance of the photocatalytic process can be significantly improved by thermal assistance.^[19] As reported, Xuan’s group developed a system where nano-sized CuO-ZnO-Al₂O₃ was used as catalyst and in the system, the methanol aqueous solution was vaporized via photo-thermo effect of catalyst for solar-driven thermo-reforming of methanol. They found that the gas phase reactants wrapping the catalyst could effectively reduce the heat loss from the catalyst and the vaporization of the methanol aqueous solution via photo-thermo conversion of catalyst took up much heat from the catalyst.^[22] Typically, the catalyst should have a broad-spectrum absorbability and higher photo-thermal conversion efficiency. Recently, surface plasmon resonance (SPR) metals, such as Au, Ag and Cu, have currently attracted much attention because the full-spectrum of sunlight can be utilized by SPR nano-catalyst compared with the traditional photocatalysts.^[23-26] It could generate energetic hot carriers through the excitation by the

School of Chemical Engineering and Technology, Xi’an Jiaotong University, Xi’an 100190, China

*E-mail: sunjie@xjtu.edu.cn (J. Sun)

localized surface plasmon resonance (LSPR) effect which can locally heat the nano-catalyst to drive the thermocatalytic reaction process.^[27] It is predictable that this LSPR effect can effectively increase the reaction temperature of photo-reforming process.^[28] Among the SPR metals, Cu has more application potential due to satisfying performance and low cost.^[29,30] In addition, Cu-based catalysts have shown excellent performance for H₂ production by methanol thermo-reforming^[31] and methanol photo-reforming.^[32,33] In general, the oxidation states of copper (i.e., Cu⁽⁰⁾, Cu⁺, and Cu²⁺) can be varied under UV irradiation.^[34-36]

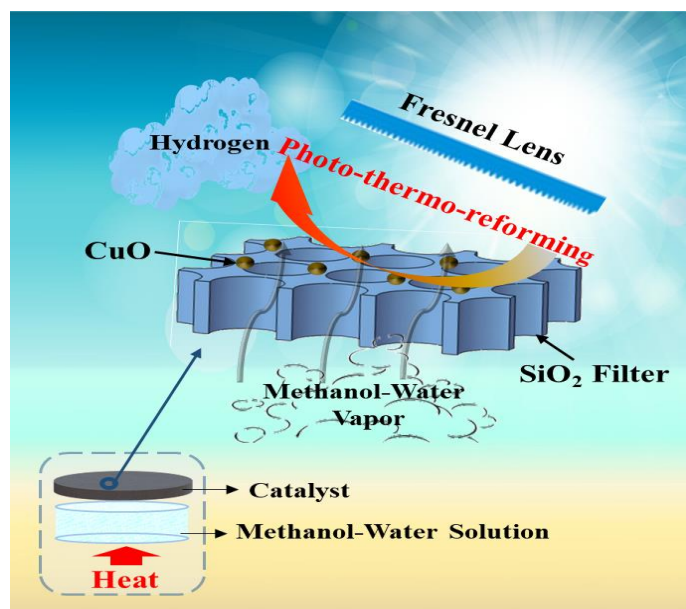


Fig. 1 Schematic diagram of solar-driven photo-thermo-reforming of methanol for hydrogen production.

Based on what is aforementioned, in the present work, we developed a reaction system for high-efficient and low-cost solar-driven hydrogen production through photo-thermo-reforming using commercial CuO as catalyst. As shown the Fig.1, we loaded the CuO catalyst on the SiO₂ membrane and suspended it above the methanol aqueous surface. The methanol aqueous was heated to generate the methanol and water mixed steams as the reactants. In this way, the chemical reaction is guaranteed to proceed in complete gas-phase, which is beneficial to the photo-thermo-reforming. In the system, catalyst nanoparticles are wrapped in the mixed steam so that all the heat generated by the catalyst is used for the chemical reaction. Under 15 suns irradiance, the surface temperature of catalyst achieves 220 °C. The commercial CuO exhibits an enhanced H₂ production rate of 100.33 m mol g⁻¹ h⁻¹, which is 334 times of that in liquid photo-reforming under the same irradiance. The hydrogen production enhancement can be attributed to the efficient utilization of the solar heat flux and the photo-thermal property of the CuO-based catalyst under the concentrated irradiation.

2. Results and discussion

2.1 Characterization and experiment

Here, X-Ray Diffraction (XRD) pattern was performed to assess the crystalline properties of catalyst. Fig. 2 shows the XRD patterns of fresh CuO, used CuO and reference CuO. It is seen that all the crystal diffraction peaks are consistent with the standard card (48-1548), which suggests that the crystal of sample is in monoclinic phase. It is worth noting that the location of the diffraction peak of CuO shifts slightly toward the large angle after the reaction, which indicates that the used CuO has a narrower interplanar crystal spacing. This could be attributed to more crystal defects in the copper oxide after the reaction. In addition, the CuO is collected in the liquid photo-reforming process and records as reference CuO. As shown in Fig. 2, the crystal diffraction peaks of reference CuO are consistent with the fresh CuO, which could suggest that CuO is not reduced during the liquid phase reaction.

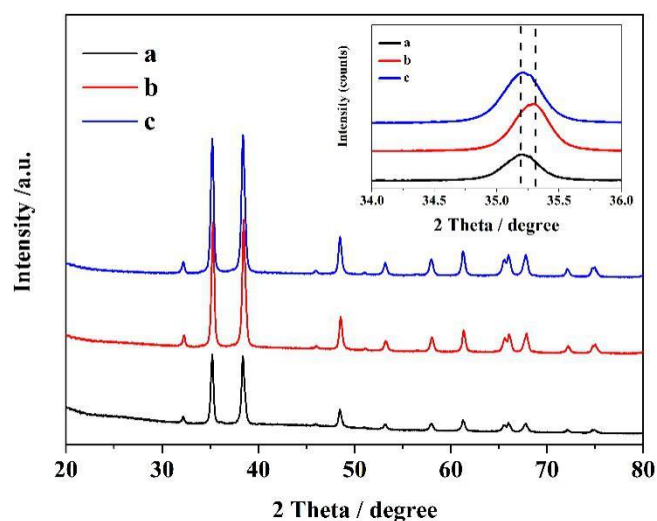


Fig. 2 XRD pattern: a) fresh CuO, b) used CuO, c) reference CuO.

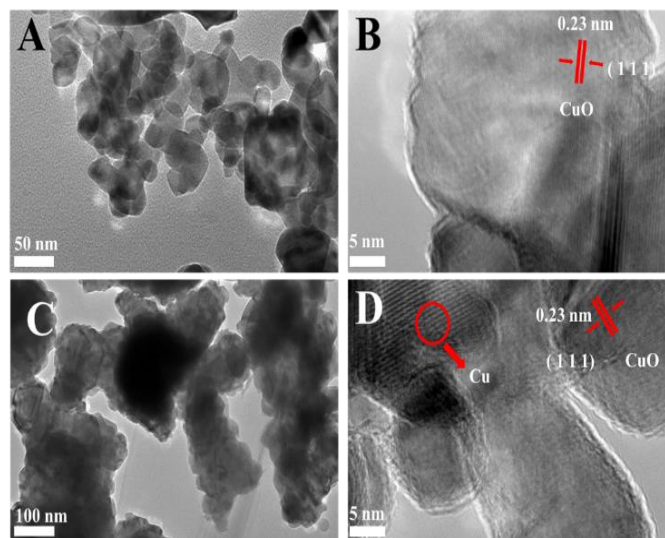


Fig. 3 A) TEM of fresh CuO; B) HRTEM of fresh CuO; C) TEM of CuO after 30 min reaction; and D) HRTEM of CuO after 30 min reaction.

As shown in Fig. 3A, the fresh CuO exhibits sphere-like nanoparticle structure with the diameter of about 40 nm. From Fig. 3B, we can clearly see the lattice fringe image of fresh CuO. The interplanar crystal spacing of (1 1 1) crystallographic plane of fresh CuO is 0.23 nm, which is consistent with the results of XRD pattern and previous report.^[37] As shown in Fig. 3C, the TEM of CuO after 30 min reaction shows nanoparticle agglomerates, which are due to the agglomeration of the catalyst in the high temperature environment. From Fig. 3D, a wider lattice fringes can be seen, which should belong to the element Cu. Above results indicate that the element Cu with SPR effect can appear during the reaction process.

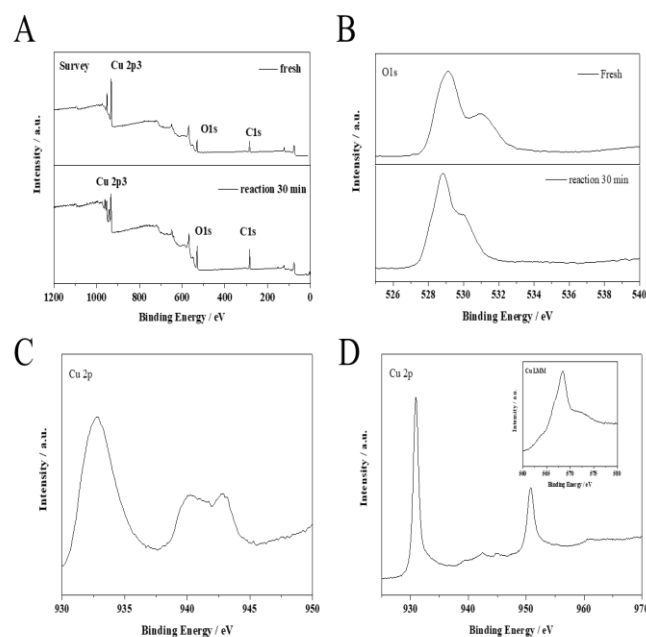


Fig. 4 XPS analysis: A) Survey spectrum for fresh CuO and after 30-min reaction CuO; B) O 1s spectra for fresh CuO and reaction 30 min CuO; C) Cu 2p spectrum for fresh CuO; D) Cu 2p spectrum (inset: Cu LMM Auger) for CuO after 30 min reaction.

In order to further understand the chemical composition of the active components in the photo-thermo-reforming process, the variations of the oxidation states of CuO surface during the reaction were analyzed through the surface photoelectron spectrum (XPS). The catalysts were collected after 30 min reaction and the sample was prepared in a vacuum chamber. From the survey curves of the samples in Fig. 4A, copper, oxygen and carbon can be clearly seen in the fresh CuO and that after 30-min reaction. Note that the carbon peaks may attribute to the impurities during the machine detection process. Fig. 4B shows that the peak area of lattice oxygen decreases significantly after 30-min reaction, which may be due to toward surface migration of lattice oxygen by photo-thermal process. Fig. 4C shows double peaks located at 935.2 and 943 eV of Cu 2p of fresh CuO, which should belong to the Cu⁽²⁾.^[20] In addition, double

peaks of the copper 2p spectrum can be clearly seen from Fig. 4D. The peaks located at 931.8 and 952.7 eV could belong to the Cu⁽¹⁾ or Cu⁽⁰⁾ after 30-min reaction.^[32] Indeed, from the Cu LMM Auger of CuO after 30 min reaction it is predictable that only Cu⁽⁰⁾ exists.

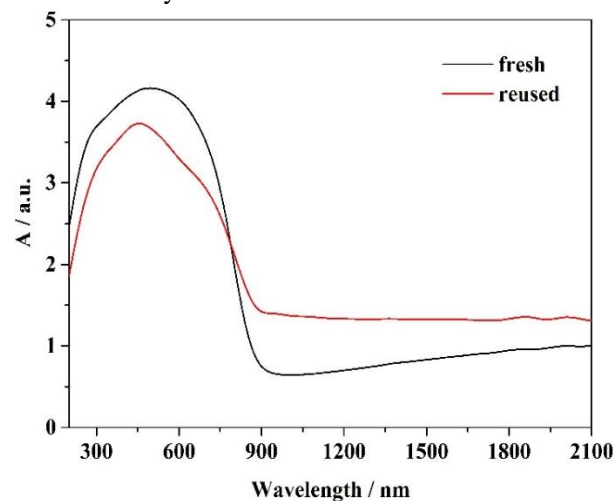


Fig. 5 UV -Vis-IR spectra of fresh CuO and reused CuO.

UV-Vis diffuse reflection was used to characterize the light absorbability of the fresh CuO and used CuO. As shown in Fig. 5, after the reaction, the light absorption range of the catalyst has been significantly broadened. This may be due to the SPR effect of Cu element.^[20] Here, the hydrogen production rates were compared between methanol photo-reforming and photo-thermo-reforming under 15 suns irradiance. The methanol photo-reforming was performed with CuO powder suspension. As shown in Fig. 6, the hydrogen production rate of methanol photo-reforming is 0.33 m mol g⁻¹ h⁻¹ while that of methanol photo-thermo-reforming achieves 100.33 mmol g⁻¹ h⁻¹. This excellent catalytic performance comes from efficient utilization of full-spectrum sunlight in the proposed reaction system, where the thermal assistance must play an essential role.

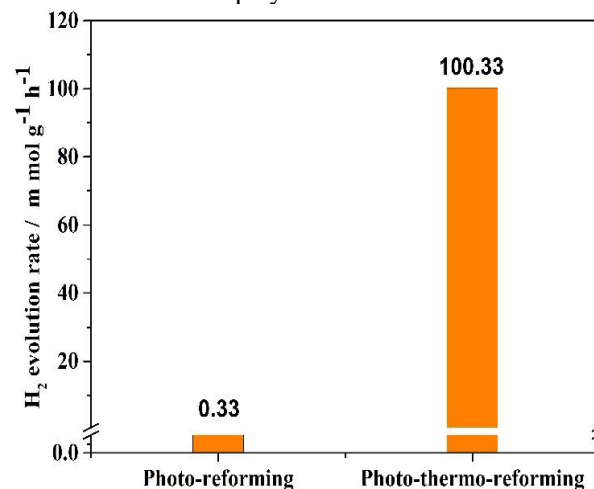


Fig. 6 Comparison of H₂ production rate between methanol photo-reforming and photo-thermo-reforming under 15-sun irradiance (1 sun = 1 kW/m²).

Next, the effect of irradiance on the hydrogen production performance was explored. Meanwhile, the reaction temperature was also recorded. As shown in Fig. 7A, the hydrogen production performance of the catalyst shows an upward trend with the increase of light intensity. Meanwhile, as shown in Fig. 7B, under 10, 15 and 20 suns irradiances, the corresponding equilibrated reaction temperature are 185, 220 and 260 °C, respectively. It is worth mentioning that this work achieved 220 °C under 15 suns irradiance for hydrogen production from methanol reforming. This indicates that the reaction has reached the reaction temperature of methanol reforming (250 °C), which indicates that the reaction at this time is mainly a thermal reaction. It is worth mentioning that we achieved 185 °C of reaction temperature and 72.8 m mol g⁻¹ h⁻¹ of H₂ production rate under 10 suns, however, no hydrogen production under the same irradiance with the same amount of CuO catalyst reported in a late reference of similar work.^[22] Therefore, temperature is a key factor affecting the activity of the catalyst under 10 to 15 suns. Higher temperature means better hydrogen production performance in the methanol photo-reforming reaction. This excellent hydrogen production performance validates the design guidance of our reaction system.

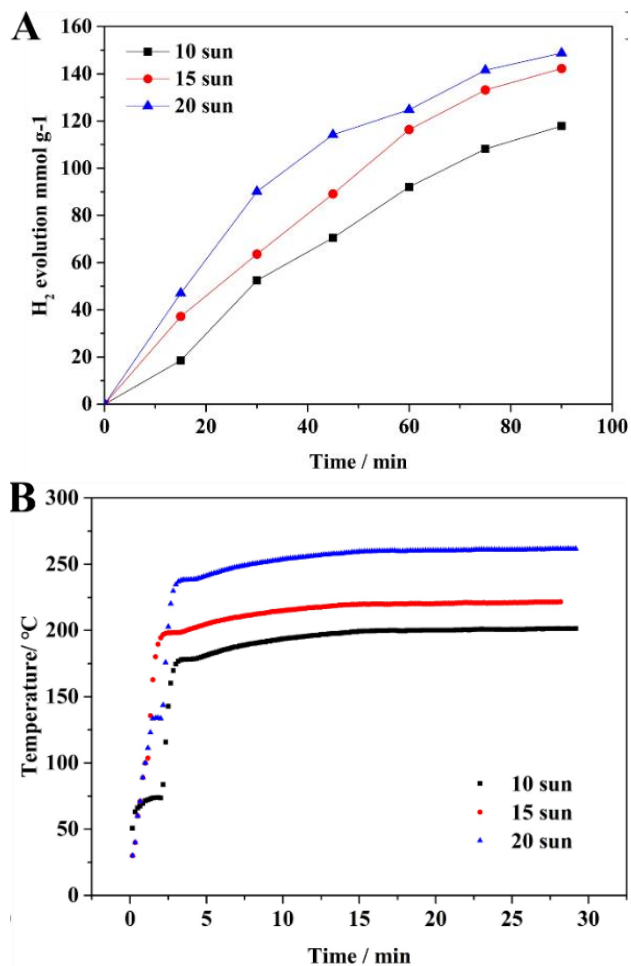


Fig. 7 A) H₂ evolution against time under different irradiance, and B) catalyst temperature against reaction time under different irradiances.

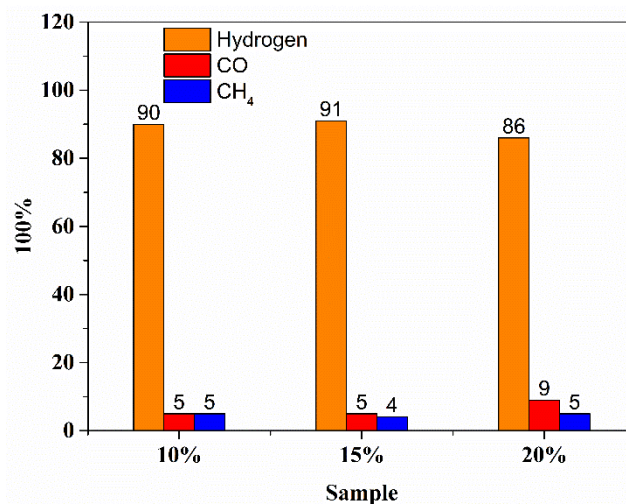


Fig. 8 Effect of methanol-water ratio on hydrogen selectivity.

For the hydrogen production from methanol reforming reaction, the ratio of methanol to water is one of the most important parameter that determines the selectivity of hydrogen. Therefore, it is necessary to explore the composition of gas components under different methanol-water ratios. Except for changing the volume fraction of methanol aqueous solution, other conditions remained the same under 15 suns irradiance. As shown in Fig 8, when the volume fractions of methanol are 10%, 15% and 20%, the proportion of hydrogen holds above 85%, where the highest proportion of hydrogen up to 91% is found when the volume fractions of methanol is 15%.

As shown in Fig. 9, the present CuO catalyst does not show an obvious deactivation in H₂ production performance after 4 cycles, indicating high catalytic stability. Since a part of CuO has been proved to be on-situ reduced into the element Cu in the present reaction system for thermal assistance by LSPR effect, it is worth mentioning that CuO can be used directly into the reaction system without being pre-reduced, which makes it economically and technologically more competitive for the application of H₂ production by methanol photo-thermo-reforming.

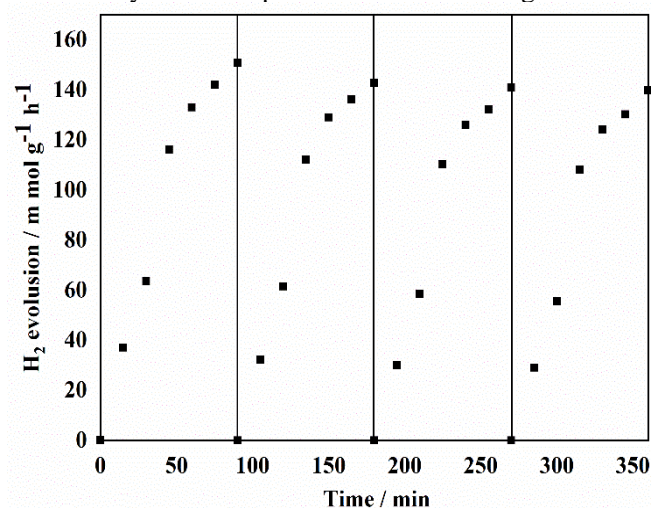


Fig. 9 Cyclic test.

2.2 Mechanism

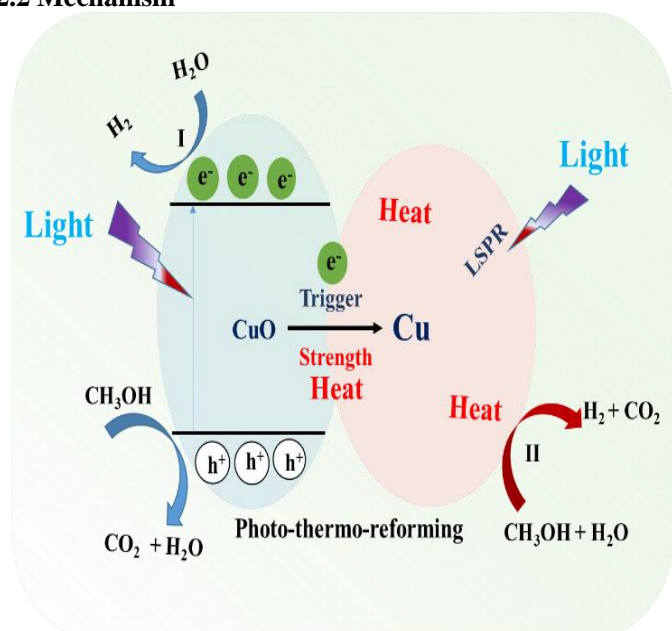


Fig. 10 Schematic presentation of photo-thermo-catalytic synergism.

Here, the mechanism of CuO for the photo-thermo-catalytic system was explored and proposed. The conversion process of CuO reduced to Cu is shown in Fig. 10. Firstly, under the excitation of light, CuO could generate lots of electrons and holes. Then, electrons can reduce water to produce hydrogen and the holes are captured by methanol. Secondly, under concentrated irradiation, the electrons can reduce $\text{Cu}^{(2)}$ to $\text{Cu}^{(0)}$, i.e. the element Cu. Finally, the LSPR effect of element Cu increases the local temperature of catalyst, which accelerates CuO to be reduced to the element Cu by increasing the efficiency of lattice oxygen migration toward the surface of CuO. Therefore, the enhanced hydrogen production in the reaction process can be divided into two pathways. Before the appearance of element Cu, the hydrogen production is mainly driven by the photocatalytic property of CuO as the Pathway I shown in blue in Fig. 10. Indeed, the heating curve of the catalyst (Fig. 7B) shows that Pathway I mainly exists in the first 10 minutes of the reaction process. After the appearance of element Cu, hydrogen production is mainly driven by the properties of photothermocatalysis and thermocatalysis of element Cu as the Pathway II shown in red in Fig. 10.^[20] It is noteworthy that CuO is hardly reduced to elemental Cu in the methanol photo-reforming, where the reaction is completely occurring in liquid phase. Therefore, the photo-thermo-reforming methanol process (Pathway II) driven by elemental Cu is the main reason for the enhanced performance of hydrogen production. To conclude, as schematically elucidated in Fig. 10, the present photo-thermo-catalytic synergism in the methanol reforming process can be comprehended as a self-promoting cycle triggered by in-situ photoreduction of CuO into element Cu and enhanced by the thermally LSPR effect of element Cu.

3. Conclusion

In the present work, we proposed a novel reaction system for high-efficient and low-cost hydrogen production by solar-driven photo-thermo-reforming gas reforming of methanol using commercial CuO as catalyst and beneficial from the photo-thermo-catalytic synergism under concentrated irradiation. In the proposed system, the CuO catalyst was loaded on the SiO_2 membrane and suspended above the heated methanol aqueous to guarantee the chemical reaction to proceed in a complete gas-phase, which is beneficial to the photo-thermo-reforming. Under 15-sun irradiance, the temperature of the catalyst can achieve $220\text{ }^\circ\text{C}$ and the hydrogen production rate reaches $100.33\text{ m mol g}^{-1}\text{ h}^{-1}$, which is 304 times higher than that reported in the late reference. When 100 mg catalyst is used, the solar-to-hydrogen efficiency can reach up to 1.85%. The remarkable performance is attributed to the photo-thermo-catalytic synergism. Based on a series of characterizations and analyses, the present photo-thermo-catalytic synergism in the methanol reforming process is revealed as a self-promoting cycle triggered by in-situ photoreduction of CuO into element Cu and enhanced by the thermally LSPR effect of element Cu.

4. Experimental section

4.1 Preparation and characterization of catalyst

Spherical copper oxide with a particle size of 40 nm was purchased from Shanghai Macklin Co., Ltd.. SiO_2 fiber membrane was purchased from Germanmucktell Co., Ltd. Methanol was purchased from Tianjin Fuyu Chemical Co., Ltd. All the water used in this experiment is deionized water. 100 mg of CuO was dispersed in 20 mL of deionized water, and then sonicated to form a uniformly dispersed suspension. Next, the copper oxide suspension was spin-coated on the silicon dioxide surface to obtain a copper silicon dioxide film, and finally the film was vacuum dried at $80\text{ }^\circ\text{C}$. for two hours.

The morphologies and microstructures of the samples were observed by a high resolution transmission electron microscope (HRTEM; JEM-2100, JEOL, Japan). The crystal phase of the samples was analyzed by an X-ray diffractometer (XRD; LabX XRD-6100, SHIMADZU, Japan) with Cu K_α radiation ($\lambda = 1.5418\text{ \AA}$). The UV-VIS-NIR diffuse reflectance spectra were recorded on a UV-VIS-NIR spectrophotometer (Lambda 950, PerkinElmer, USA). The X-ray photoelectron spectroscopy (XPS) was performed by an X-ray photoelectron spectroscope (ESCALAB Xi+, Thermo Fisher, USA) with the $\text{C}1s=284.8\text{ eV}$ as binding energy standardization.

4.2 Photo-thermo-reforming experiment

All experiments were carried out in a closed Pyrex top-irradiation vessel. The catalyst-loaded SiO_2 membrane was placed above the methanol aqueous solution. Methanol aqueous solution was vaporized and then contacted with

catalyst for reaction. A 70°C constant temperature oil bath (B11-1, Shanghai, Si Le, China) was used to provide heat for the vaporization of methanol solution. A 300 W Xe lamp (CEL-PE300-3A, Beijing Teach Jinyuan Technology, China) was used as the experimental light source to simulate sunlight with various irradiances by adjusting the current. The irradiance was measured by an optical power and energy meter (PM100D, Thorlabs, USA). The products of gas were evaluated by an online gas chromatograph (GC9790II, Fuli Instruments, China) equipped with thermal conductive detector (TCD) and flame detector (FID), using argon as carrier gas. In a typical experiment, firstly, 50 mL of methanol aqueous solution with 10% volume fraction was placed in a reactor. Next, light source was turned on to start the reaction when the temperature of the solution reached 70°C. All experiments were performed in nitrogen atmosphere. The temperature of the dark side membrane was monitored by K-type thermocouple connected to DAQ system (Agilent 34972A with 34901A, USA).

4.3 Solar energy utilization efficiency

The calculation method of solar energy to hydrogen energy is consistent with Xuan's group report as shown in Equation (1).

$$\eta = \frac{\Delta H \cdot C_{H_2} / 3}{IA + Q} \quad (1)$$

where C_{H_2} refers to the hydrogen production rate that is equal to 100.33 m mol g⁻¹ h⁻¹. I refers to the solar irradiation intensity that is 15000 W/m². A is the area of the catalyst receiving light that is 0.001256 m². ΔH is equal to 126.7 kJ/mol⁻¹, and Q is the heat power of vaporization of methanol and water required for the reaction that is 0.198 W.

Acknowledgements

This work was financially supported by the National Natural Science Foundation of China (51776196), the Natural Science Foundation of Shaanxi Province (2020JM-048), the Shaanxi Creative Talents Promotion Plan-Technological Innovation Team (2019TD-039), the Foshan Xianhu Laboratory of the Advanced Energy Science and Technology Guangdong Laboratory (XHD2020-001), and Fundamental Research Funds for the Central Universities.

Supporting information

Applicable, <https://dx.doi.org/10.30919/esee8c722>

Conflict of interest

The authors declare that they have no known competing financial interests or personal relationships that could have appeared to influence the work reported in this paper.

References

- [1] M. Z. Jacobson, W. G. Colella and D. M. Golden, *Science*, 2005, **308**, 1901-1905, doi: 10.1126/science.1109157.
- [2] I. Staffell, D. Scamman, A. V. Abad, P. Balcombe, P. E. Dodds, P. Ekins, N. Shah and K. R. Ward, *Energy Environ. Sci.*, 2019, **12**, 463-491, doi: 10.1039/c8ee01157e.
- [3] M. T. Zhao, K. Yuan, Y. Wang, G. D. Li, J. Guo, L. Gu, W. P. Hu, H. J. Zhao and Z. Y. Tang, *Nature*, 2016, **539**, 76-80, doi: 10.1038/nature19763.
- [4] C. Corgnale, B. Hardy, T. Motyka, R. Zidan, J. Teprovič and B. Peters, *Renew. Sust. Energy Rev.*, 2014, **38**, 821-833, doi: 10.1016/j.rser.2014.07.049.
- [5] N. Armaroli and V. Balzani, *ChemSusChem*, 2011, **4**, 21-36, doi: 10.1002/cssc.201000182.
- [6] Y. S. H. Najjar, *Int. J. Hydrog. Energy*, 2013, **38**, 10716-10728, doi: 10.1016/j.ijhydene.2013.05.126.
- [7] B. L. Dou, H. Zhang, Y. C. Song, L. F. Zhao, B. Jiang, M. X. He, C. J. Ruan, H. S. Chen and Y. J. Xu, *Sustain. Energy Fuels*, 2019, **3**, 314-342, doi: 10.1039/c8se00535d.
- [8] M. Luo, Y. Yi, S. Z. Wang, Z. L. Wang, M. Du, J. F. Pan and Q. Wang, *Renew. Sust. Energy Rev.*, 2018, **81**, 3186-3214, doi: 10.1016/j.rser.2017.07.007.
- [9] B. Han and Y. H. Hu, *Energy Sci. Eng.*, 2016, **4**, 285-304, doi: 10.1002/ese3.128.
- [10] L. L. Lin, W. Zhou, R. Gao, S. Y. Yao, X. Zhang, W. Q. Xu, S. J. Zheng, Z. Jiang, Q. L. Yu, Y. W. Li, C. Shi, X. D. Wen and D. Ma, *Nature*, 2017, **544**, 80-83, doi: 10.1038/nature21672.
- [11] R. E. Rodriguez-Lugo, M. Trincado, M. Vogt, F. Tewes, G. Santiso-Quinones and H. Grutzmacher, *Nat. Chem.*, 2013, **5**, 342-347, doi: 10.1038/nchem.1595.
- [12] M. A. Mehmood, M. Ibrahim, U. Rashid, M. Nawaz, S. Ali, A. Hussain and M. Gull, *Sustain. Prod. Consump.*, 2017, **9**, 3-21, doi: 10.1016/j.spc.2016.08.003.
- [13] C. F. Shih, T. Zhang, J. Li and C. Bai, *Joule*, 2018, **2**, 1925-1949, doi: 10.1016/j.joule.2018.08.016.
- [14] E. A. Kozlova and V. N. Parmon, *Russ. Chem. Rev.*, 2017, **86**, 870-906, doi: 10.1070/RCR4739.
- [15] G. Colon, *Appl. Cat. A*, 2016, **518**, 48-59, doi: 10.1016/j.apcata.2015.11.042.
- [16] S. Obregón, M. J. Muñoz-Batista, M. Fernández-García, A. Kubacka and G. Colón, *Appl. Cat. B.*, 2015, **179**, 468-478, doi: 10.1016/j.apcatb.2015.05.043.
- [17] A. Caravaca, H. Daly, M. Smith, A. Mills, S. Chansai and C. Hardacre, *React. Chem. Eng.*, 2016, **1**, 649-657, doi: 10.1039/c6re00140h.
- [18] U. Caudillo-Flores, G. Agostini, C. Marini, A. Kubacka and M. Fernandez-Garcia, *Appl. Cat. B.*, 2019, **256**, 117790, doi: 10.1016/j.apcatb.2019.117790.
- [19] V. Nair, M. J. Muñoz-Batista, M. Fernandez-Garcia, R. Luque and J. C. Colmenares, *Chem. sus. Chem.*, 2019, **12**, 2098-2116, doi: 10.1002/cssc.201900175.
- [20] L. Zhao, Y. Qi, L. Song, S. Ning, S. Ouyang, H. Xu and J. Ye, *Angew. Chem. Int. Edit.*, 2019, **58**, 7708-7712, doi: 10.1002/anie.201902324.
- [21] J. J. Li, E. Q. Yu, S. C. Cai, X. Chen, J. Chen, H. P. Jia and Y. J. Xu, *Appl. Cat. B.*, 2019, **240**, 141-152, doi: 10.1016/j.apcatb.2018.08.069.
- [22] X. Yu, J. Zeng and Y. Xuan, *Energy Technol.*, 2019, **7**, 1900299, doi: 10.1002/ente.201900299.
- [23] Y. Sivan, J. Baraban, I. W. Un and Y. Dubi, *Science*, 2019, **364**, eaaw9367, doi: 10.1126/science.aaw9367.

- [24] C. Kim, B. L. Suh, H. Yun, J. Kim and H. Lee, *ACS Catal.*, 2017, **7**, 2294-2302, doi: 10.1021/acscatal.7b00411.
- [25] D. Gao, W. Liu, Y. Xu, P. Wang, J. Fan and H. Yu, *Appl. Catal. B*, 2020, **260**, 118190, doi: 10.1016/j.apcatb.2019.118190.
- [26] X. Meng, L. Liu, S. Ouyang, H. Xu, D. Wang, N. Zhao and J. Ye, *Adv. Mater.*, 2016, **28**, 6781-6803, doi: 10.1002/adma.201600305.
- [27] M. Q. Yang, L. Shen, Y. Lu, S. W. Chee, X. Lu, X. Chi, Z. Chen, Q. H. Xu, U. Mirsaidov and G. W. Ho, *Angew. Chem. Int. Edit.*, 2019, **58**, 3077-3081, doi: 10.1002/anie.201810694.
- [28] J. X. Chen, J. Feng, F. Yang, R. Aleisa, Q. Zhang and Y. D. Yin, *Angew. Chem. Int. Edit.*, 2019, **58**, 9275-9281, doi: 10.1002/anie.201904828.
- [29] X. Y. Gan, E. L. Keller, C. L. Warkentin, S. E. Crawford, R. R. Frontiera and J. E. Millstone, *Nano Lett.*, 2019, **19**, 2384-2388, doi: 10.1021/acs.nanolett.8b05088.
- [30] J. Jiao, R. Lin, S. Liu, W.C. Cheong, C. Zhang, Z. Chen, Y. Pan, J. Tang, K. Wu, S.F. Hung, H. M. Chen, L. Zheng, Q. Lu, X. Yang, B. Xu, H. Xiao, J. Li, D. Wang, Q. Peng, C. Chen and Y. Li, *Nat. Chem.*, 2019, **11**, 222-228, doi: 10.1038/s41557-018-0201-x.
- [31] A. Carrero, J. A. Calles and A. J. Vizcaino, *Appl. Catal.*, 2007, **327**, 82-94, doi: 10.1016/j.apcata.2007.04.030.
- [32] A. López-Martín, F. Platero, A. Caballero and G. Colón, *Chem. Phot. Chem.*, 2020, **4**, 630-637, doi: 10.1002/cptc.202000010.
- [33] F. Coloma, F. Marquez, C. H. Rochester and J. A. Anderson, *Phys. Chem. Chem. Phys.*, 2000, **2**, 5320-5327, doi: 10.1039/b005331g.
- [34] M. Jung, J. Scott, Y. H. Ng, Y. J. Jiang and R. Amal, *Int. J. Hydrog. Energy*, 2014, **39**, 12499-12506, doi: 10.1016/j.ijhydene.2014.06.020.
- [35] D. Guerrero-Araque, P. Acevedo-Pena, D. Ramirez-Ortega, H. A. Calderon and R. Gomez, *Int. J. Hydrog. Energy*, 2017, **42**, 9744-9753, doi: 10.1016/j.ijhydene.2017.03.050.
- [36] D. M. Tobaldi, N. Rozman, M. Leoni, M. P. Seabra, A. S. Skapin, R. C. Pullar and J. A. Labrincha, *J. Phys. Chem. C*, 2015, **119**, 23658-23668, doi: 10.1021/acs.jpcc.5b07160.
- [37] G. Kalaiyan, S. Suresh, S. Thambidurai, K. M. Prabu, S. K. Kumar, N. Pugazhenthiran and M. Kandasamy, *J. Mol. Struct.*, 2020, **1217**, 128379, doi: 10.1016/j.molstruc.2020.128379

Publisher's Note: Engineered Science Publisher remains neutral with regard to jurisdictional claims in published maps and institutional affiliations.